Journal of Thermal Analysis and Calorimetry, Vol. 88 (2007) 3, 885–891

THERMAL DECOMPOSITION AND ELECTRON MICROSCOPY STUDIES OF SINGLE-WALLED CARBON NANOTUBES

A. W. Musumeci[1], *G. G. Silva*[2], *W. N. Martens*[1], *E. R. Waclawik*[1] *and R. L. Frost*[1*]

[1]Inorganic Materials Research Program, School of Physical and Chemical Sciences, Queensland University of Technology GPO Box 2434, Brisbane Queensland 4001, Australia
[2]Departamento de Química, Universidade Federal de Minas Gerais, Pampulha, Belo Horizonte 31270-901, Minas Gerais, Brazil

Thermoanalytical and electron microscopic methods were used as characterisation tools for the determination of the composition of single walled carbon nanotube samples. Acid purification method of single-walled carbon nanotubes (SWCN) proved to be effective, resulting in a three fold increase in the percentage of SWNTs present in the purified product as determined by thermogravimetric analysis. In this work we report the thermogravimetric analysis by conventional and high resolution methods of the raw SWNTs and purified SWNTs.

Keywords: *high resolution thermogravimetry, purification, single walled carbon nanotubes, thermal analysis*

Introduction

Since the work of Iijima [1] in 1991, carbon nanotubes have been the subject of significant attention for many research scientists. They are a unique nanostructured material that can be considered conceptually as one-dimensional quantum wires. Carbon nanotubes have remarkable thermal, electronic and mechanical properties [2, 3] stemming from their structural similarity to graphene sheets and their one-dimensionality. The single walled carbon nanotube is the simplest form of nanotube and can be visualised as a single sheet of graphene rolled-up into a steamless tube that may be several microns in length and as small as 0.7 nm in diameter [4]. Carbon nanotubes are either metallic or semiconducting in nature depending on their chirality and diameter, thus making them ideal reinforcing fillers in composite materials. Polymer composites containing carbon nanotubes are of great interest as they may possess new or novel combinations of electrical, optical and mechanical properties [5, 6].

Carbon nanotubes synthesised by common techniques such as arc discharge [1, 7], laser vaporisation [8] and catalytic pyrolysis [9] often yield a randomly entangled array of metal catalyst particles, nanotubes and other carbonaceous materials which require post-synthesis manipulation. Arc discharge synthesis is used in the large scale production of carbon nanotubes [10] which often requires significant purification and work-up for many applications because the as-produced material frequently contains a significant content of impurities [11]. Several catalysts have been used to synthesize SWNT through arc discharge, the morphology and ratio of catalyst, the mechanism of nanotube growth and the properties of the final soots have been extensively discussed [12, 13]. A special case of interest is the SWNT prepared by arc using Ni–Y in the ratio 4:1 at.% since this material is commercialized (by Carbolex) and widely used in fundamental an applied research [13–18].

There have been a number of significant studies in the thermal analysis of both single-walled and multi-walled carbon nanotubes [19–24]. The aim of these studies is often to characterize the purity of the carbon material treated by several different procedures. Thermal analysis has also been used to study the properties of composites with carbon nanotube filler [25–27].

Some of the best reports of purity evaluation in the literature employed conventional TG performed at 5°C min^{-1} in air [11, 13, 19, 21–23]. The general behaviour summarized in Fig. 1 can be extracted from these reports. The temperature of maximum rate of decomposition assigned to carbon nanotube fraction

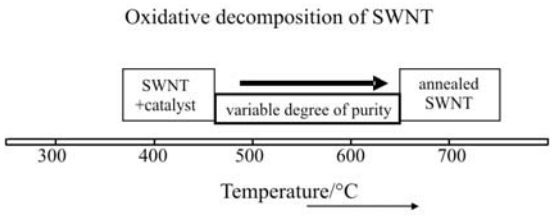

Fig. 1 Flow chart of the temperature range for the oxidation of SWNT based on thermogravimetric studies at 5°C min^{-1} in air [11, 19, 21–23]

* Author for correspondence: r.frost@qut.edu.au

1388–6150/$20.00

Akadémiai Kiadó, Budapest, Hungary
Springer, Dordrecht, The Netherlands

in SWNT and MWNT can vary from 390 to 730°C depending on the content of metal catalyst and more reactive carbonaceous materials. The structure of the nanotube walls also influences the results, annealed samples with lower content of defects and functionalities exhibit higher thermal stability.

The as-bought carbon nanotubes employed in this work were of stated 50–70 vol% purity. However, it is reported to be very difficult to extract this amount of nanotube from the commercial raw material, after the purification procedures [19]. The purpose of this work is to attain a better understanding of the exact composition of purified and unpurified SWNT matrices through thermogravimetric analysis. TG methods of high resolution thermogravimetry (HRTG) [28, 29] were used to this purpose.

Experimental

Purification of SWNTs

Purification of the single-walled carbon nanotubes was undertaken using a method adopted from Furtado *et al*. [17]. The as-prepared SWNTs (Carbolex) was heated in a furnace under air at 395°C for 20 min. After this stage of dry oxidation the material was refluxed in 3.0 mol L^{-1} HCl for 4 h. The acidified dispersion was then filtered through polycarbonate membranes and copiously washed with ultra-pure water (Milli-Q). The filtrate was twice resuspended in water, sonicated, filtered and washed with ultra-pure water. These procedures led to loss of material at each stage. The yield of the purification was 6 mass%.

Scanning electron microscopy (SEM)

Samples were prepared for SEM by dropping sonicated DMF dispersions of carbon nanotubes onto an aluminium stub. The SEM images were obtained using a FEI Quanta 200 scanning electron microscope operating at 30 kV.

Thermal analysis

Thermal analyses of the carbon nanotube samples were carried out in a TA® Instruments Inc. high-resolution thermogravimetric analyser (series Q500) in a flowing air atmosphere (60 cm^3 min^{-1}). Approximately 5 mg of sample was heated in an open platinum crucible up to 1000°C with different procedures: *i*) conventional TG at rate of 5.0°C min^{-1}; *ii*) high resolution measurement (HRTG) at 10.0°C min^{-1} with resolution 6, sensitivity 1 and 4. Measurements for each sample under these conditions were performed in duplicate. Derivative thermogravimetric (DTG) curves were generated with approximately 2.000 points for the conventional TG and 6.000 points for the HRTG. The data was analysed by non-linear least squares fit to multiple Gaussian curves; the minimum number of curves was used to fit each DTG until the adjustment was judged visually satisfactory and the Pearson r^2 value was in general higher than 0.99.

Results and discussion

Scanning electron microscopy

The single-walled carbon nanotubes purchased from Carbolex have a mean diameter of 1.4 nm and are reported to aggregate into bundles of typically 100–400 SWNTs that are approximately 1–5 μm long [17, 18]. At least four different components are present in the raw materials: amorphous and graphitic forms of carbon, carbon nanotubes and metal particles that are encapsulated by carbon shells [13].

The SEM images of the as-prepared SWNTs in Fig. 2 show two typical regions. The SEM Fig. 2a focuses on a gap in the carbonaceous film of an unpurified SWNT sample. The carbon nanotube bundles imaged in Fig. 2a appear to be very thin (or even isolated nanotubes) and span the micron-sized crack in the film. Figure 2b shows a region with evidence of larger particles and aggregates that appear to have clumped together into nanotube ropes. These are similar to typical images found in literature of as-prepared soot of SWNT sample [30].

Figure 2c is an image of the purified SWNT sample. As can be noted the purified material still contains particles. The ropes are thicker and appear to be shorter. These observations can be understood in relation to the purification procedures of selective gas oxidation and acid reflux. The combustion of amorphous carbon and the digestion of the metal particles liberate the nanotubes which readily reaggregate as bundles. The SEM image in Fig. 2c indicates that the purification succeeded and a sample with higher content of carbon nanotube ropes was produced.

Thermal analysis

The unpurified SWNT materials were expected to contain approximately 20–30 mass% amorphous carbon and approximately 30 mass% of carbon coated Ni–Y particles from the catalyst [17, 18]. Therefore, the highest possible amount of SWNT in the as-prepared sample can be estimated to be approximately 50 mass%.

Thermogravimetric analysis of the unpurified SWNTs and purified SWNTs performed in conventional TG at 5°C min^{-1} in air are shown in Fig. 3. The derivative curves of TG with respect to temperature

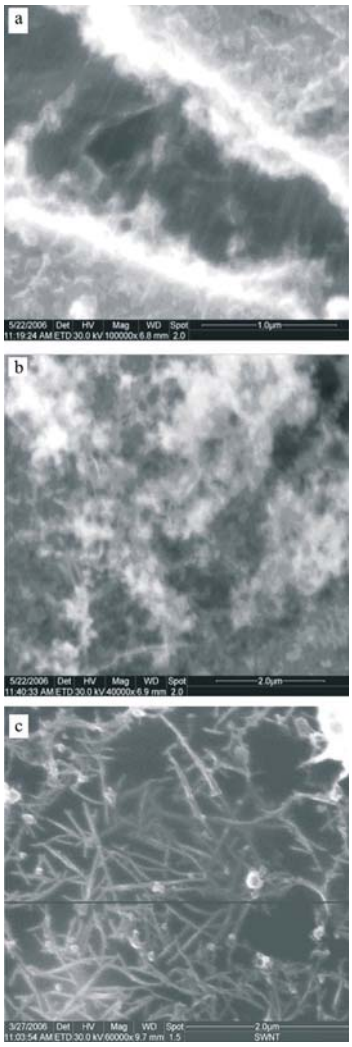

Fig. 2 SEM images of a – and b – as-prepared and c – purified SWNT

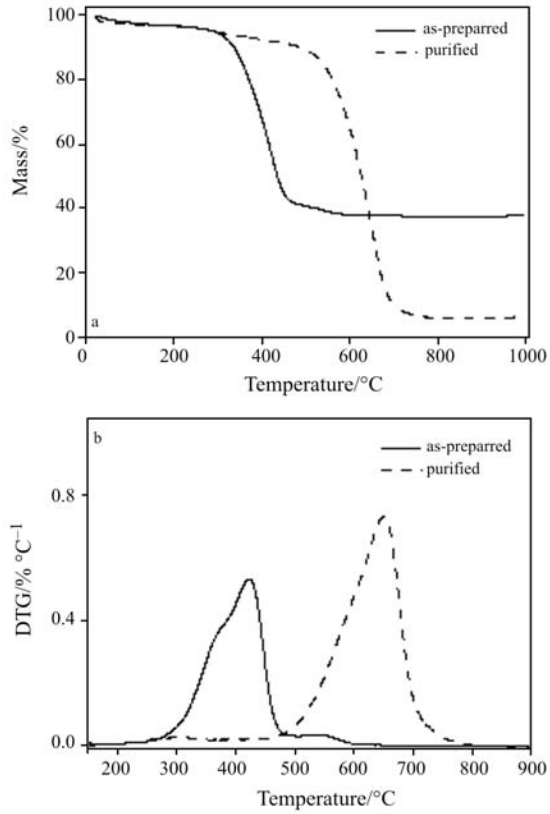

Fig. 3 a – TG and b – DTG curves obtained at 5°C min^{-1} in air for as-prepared and purified SWNTs

(DTG) (Fig. 3b) shows the shift of the temperature of maximum mass loss from 422 to 650°C after purification. The content of residue after complete thermal oxidation decreases from 38 to 7 mass% through purification. The TG residue is the oxide of the metal catalyst Ni–Y. In the case of the as-prepared material the metal catalyst oxidizes during the TG measurement. On the other hand, for the purified SWNT the purification procedure itself is likely to lead to the oxidation of catalyst metals, at least partially.

Amorphous carbon thin coating on the walls of carbon nanotubes have been observed by TEM [31]. This amorphous material should be very reactive and is considered the first fraction to oxidize during TG analysis. Amorphous fractions organized in higher particles and aggregates have been characterized as more stable materials [32] and may decompose over a larger range of temperature. Graphitic shells forming particles encapsulating the metal catalyst are more stable than the carbon nanotube fraction as observed in some works [22, 33]. Therefore, the following order of reactivity is expected for the materials present in the unpurified sample:

amorphous coating>amorphous particles>SWNT>graphitic particles

The presence of fullerenes is also reported in SWNT materials [34]. The fullerene fraction is more reactive than the carbon nanotubes [33].

Figure 4 shows TG and DTG curves for the unpurified material obtained with three different procedures. The inset in Fig. 4a exhibits the temperature program applied to the sample in each measurement. The high resolution TG curves were conducted with resolution 6 and sensitivity 1 and 4. A quasi-isothermic decomposition was performed in the experiment with sensitivity 4. The curves in Fig. 4 show that the oxidation shifts to lower temperature and the high resolution measurements are characterized by two peaks.

The association of different Gaussian lines to carbonaceous fractions in a SWNT soot was previously performed by Smith Jr. *et al*. [34]. Figure 5 presents the best results of line shape analysis with Gaussian lines for the three experimental procedures employed to study the as-prepared material. The minimum number of Gaussian lines was used to fit the experimental data. The line shape analyses were evaluated by visual inspection of the curve and take into consideration the

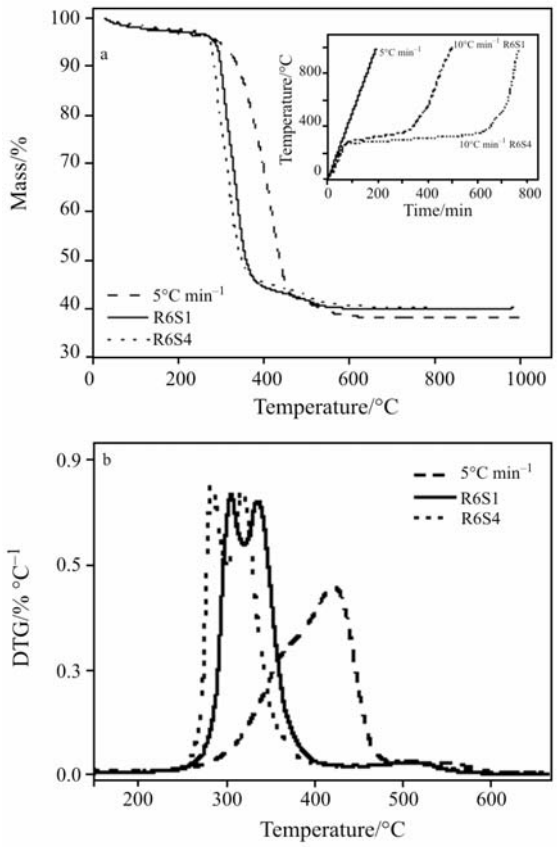

Fig. 4 a – TG and b – DTG curves for as-prepared SWNTs obtained by conventional TG at 5°C min^{-1} and by high resolution TG at resolution 6 and sensitivity 1 and 4. Inset show the variation of temperature with time in each experiment

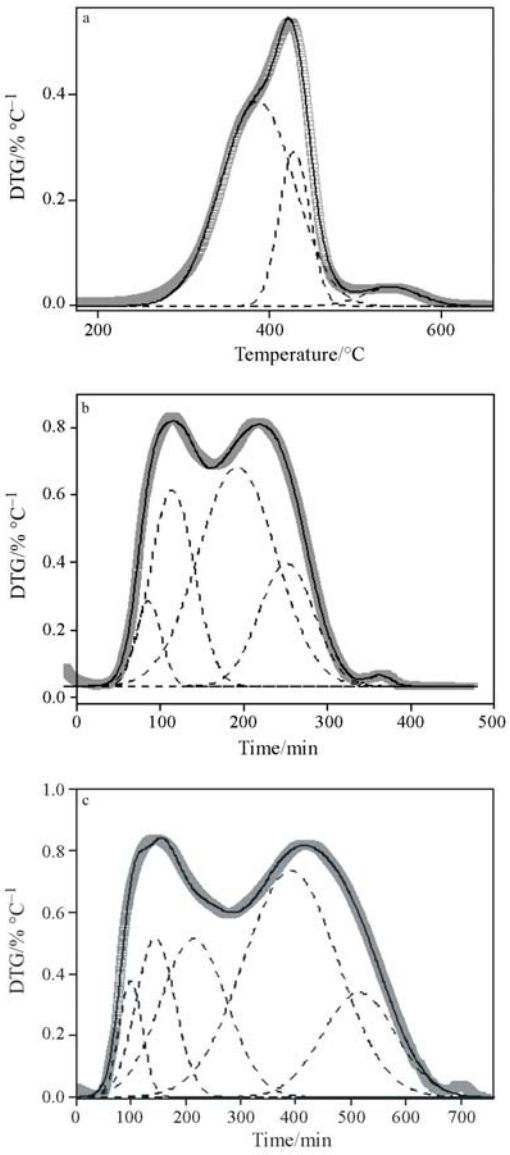

Fig. 5 DTG curves and line shape analyses for as-prepared SWNTs obtained by a – conventional TG at 5°C min^{-1} and high resolution TG at resolution 6, b – sensitivity 1 and c – 4

Pearson number r^2. Table 1 summarizes the results of the line shape analyses.

DTG curve of the conventional TG at 5°C min^{-1} was fitted with three Gaussian lines (Fig. 5a). The line at 428°C can be assigned to SWNT oxidation catalysed by the metal, as already reported [35]. This fraction decomposition occurs through approximately 35°C (full width at half maximum). Therefore, the range of temperature for a reasonable homogeneous fraction to decompose during the conventional TG at 5°C min^{-1} is ~35°C. The separate fraction decomposing around 541°C is likely to be multishell graphitic particles whose oxidation is accompanied by the mass gain of the metal particle's oxidation. The large first Gaussian line at 385°C (full width at half maximum=86°C) can not be associated with a homogeneous fraction. This mass loss peak is probably associated with amorphous carbon coating and particles and also some carbon nanotubes.

DTG curves for high resolution experiments show two major events (Figs 5b and c). All attempts to fit these curves with two Gaussian lines did not succeed. Several different functions such as Gaussian, Lorentzian, log normal were tested. Actually, there is no chemical reason to expect that the oxidation behaviour of the carbonaceous and metal fractions in the as-prepared material could be analysed considering only two mainly fractions. Therefore, the line shape analysis was performed without fixing any parameter and using the minimum number of Gaussian lines to obtain a close fit. Four Gaussian lines were deemed necessary to analyse the HRTG with resolution 6 and sensitivity 1, whereas 5 lines were required to fit the sensitivity 4 (Figs 5b and c). Table 1 shows the results of these analyses. The abrupt increase of the curves at the beginning of the oxidation, performed in quasi-isothermic conditions, was the most

Table 1 Residue and Gaussian line shape results for unpurified SWNT from TG runs obtained in air at 5°C min^{-1} and high resolution TGs with resolution 6 and sensitivity 1 and 4

Sample	1st Gaussian	2st Gaussian	3rd Gaussian	4th Gaussian	5th Gaussian	r^2	Residue/%
5°C min^{-1}	X_1=385°C W_1=86°C A_1=42%	X_2=428°C W_2=35°C A_2=13%	X_3=541°C W_3=66°C A_3=3%	–	–	0.9942	39
HRTG Sensitivity 1	X_1=103 min W_1=30 min A_1=4%	X_2=132 min W_2=52 min A_2=15%	X_3=210 min W_3=93 min A_3=29%	X_4=269 min W_4=65 min A_4=11%	–	0.9991	40
HRTG Sensitivity 4	X_1=101 min W_1=41 min A_1=3%	X_2=146 min W_2=70 min A_2=8%	X_3=215 min W_3=120 min A_3=13%	X_4=391 min W_4=170 min A_4=26%	X_5=515 min W_5=133 min A_5=10%	0.9989	40

*X_i=position, W_i=full width at half maximum and A_i=area of the Gaussian line

difficult part of the fit. The Gaussian lines in Figs 5b and c are overlapped, thus the discussion about the content of each fraction associated to these lines should be considered as an attempt to quantify an entangled oxidation behaviour.

The first two Gaussian lines on Fig. 5b and the first three lines on Fig. 5c can be assigned to amorphous fractions of the carbonaceous sample. The nature of these fractions is not possible to discuss at this level. From the work of Muller *et al*. [32] it can be affirmed that larger amorphous particles and aggregates will be more stable against oxidation than very defective thin coatings. The separate fraction which decomposes at higher temperature in the conventional TG (the peak centred at 541°C in Fig. 5a) appears to shift to lower times in the high resolution measurements and decompose mostly with the last fraction of the carbonaceous oxidation. In Fig. 5b a fifth Gaussian line (at 380 min) was assigned to this small last peak, but it corresponds to less than 1 mass% of material, thus, it is not reported in Table 1. In Fig. 5c, it was not possible to use a Gaussian line to fit the small peak around 700 min.

The carbon nanotube fraction in the experiments of Figs 5b and c corresponds to the fitted Gaussian lines centred at 210 and 391 min, respectively. Therefore, the content of carbon nanotube determined in the measurements of HRTG for the as-prepared soot is between 26–29 mass%. The last Gaussian lines of the analyses corresponding to approximately 10 mass% of the sample are assigned to more stable graphitic shells. It is possible that some content of graphitised carbon nanotube can also oxidize with this last fraction.

The drop in metal catalyst content in the purified sample was very significant (Table 2). The temperature of the dry oxidation used in the purification processes (395°C) certainly leads to the combustion of some carbon nanotubes. Lower temperatures are necessary in this step if higher yields are desired [17, 18, 23, 35]. Approximately 6 mass% of the purified material was lost before the 500°C. Figure 3 shows that some content of solvent was lost and also between 300 and 400°C there is a small mass loss.

DTG curves and line shape analyses for the purified material are shown on Fig. 6. The results for conventional TG and high resolution measurement at resolution 6 and sensitivity 1 are presented in Table 2. DTG of conventional experiment does not allow a good fit. As can be observed in Fig. 6a very large Gaussian line, passing through the base of the overall range of oxidation, is necessary to the fit. Nevertheless, important information can be extracted from Fig. 6a: the range of temperatures obtained in the decomposition, 602–655°C, is typical of purified carbon nanotubes [19, 35].

The HRTG experiment permits a better fit of the DTG curve (Fig. 6b). The three Gaussian lines can be considered as attributed to carbon nanotube fractions. This is because of the rigorous purification procedure

Table 2 Residue and Gaussian line shape results for purified SWNT from TG runs obtained in air at 5°C min^{-1} and high resolution TG with resolution 6 and sensitivity 1

Sample	1st Gaussian	2nd Gaussian	3rd Gaussian	r^2	Residue/%
5°C min^{-1}	X_1=602°C W_1=178°C A_1=27%	X_2=606°C W_2=77°C A_2=32%	X_3=655°C W_3=46°C A_3=28%	0.9864	7
HRTG Sensitivity 1	X_1=503 min W_1=35 min A_1=31%	X_2=543 min W_2=36 min A_2=41%	X_3=574 min W_3=85 min A_3=15%	0.9971	7

*X_i=position, W_i=full width at half maximum and A_i=area of the Gaussian line. **The % of material does not sum 100% because of lost of moisture or solvent and a reactive fraction (5 mass%) which decomposes from 300°C

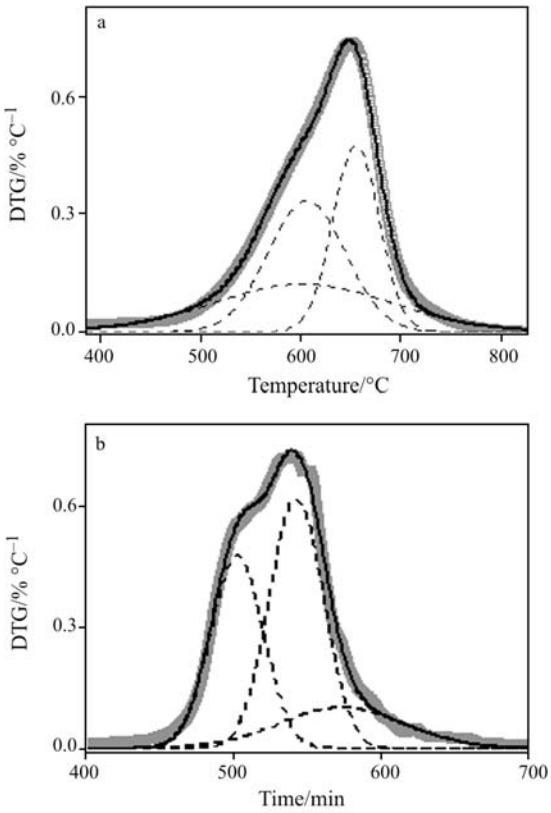

Fig. 6 DTG curves and line shape analyses for purified SWNTs obtained by a – conventional TG at 5°C min^{-1} and b – high resolution TG at resolution index 6 and sensitivity 1

employed. Although on the one hand it causes a low yield, it certainly provides a good quality material. The first Gaussian line at 503 min can be assigned to carbon nanotube combustion under influence of metal particles and to some small content of amorphous particles. The second Gaussian line at 543 min is typical of purified carbon nanotube. The third Gaussian line can be assigned to more graphitised carbon nanotube and graphitic shells. Therefore the content of carbon nanotube in the purified material can be as high as 87 mass%. The SEM images presented in Fig. 2 support qualitatively these conclusions.

Conclusions

Conventional and high resolution thermogravimetry of an unpurifed SWNT and purified SWNT matrices revealed a large amount of information regarding the accurate quantitative measurements of the content of carbonaceous by-products, carbon nanotubes, and residual metal catalyst present in the materials. Purification of the SWNTs was found to increase the content of SWNTs in the matrix by nearly 300%.

Acknowledgements

The financial and infra-structure support of the Queensland University of Technology Inorganic Materials Research Program of the School of Physical and Chemical Sciences is gratefully acknowledged. E. R. Waclawik gratefully acknowledges financial support from the United States Air Force's Asian Office of Aerospace Research and Development. Project ID: AOARD-06-4041. The Australian Research Council (ARC) is thanked for funding the thermal analysis facility. G. G. Silva thanks financial support from Brazilian agency CAPES.

References

1 S. Iijima, Nature (London), 354 (1991) 56.
2 M. M. J. E. Tracey and J. M. Gibson, Nature (London), 381 (1996) 678.
3 J. W. G. Wildoer, L. C. Venema, A. G. Rinzier, R. E. Smalley and C. Dekker, Nature (London), 391 (1998) 59.
4 M. S. Dresselhaus, G. Dresselhaus, P. C. Eklund and A. M. Rao, Phys. Chem. Mater. Low-Dimensional Struct., 23 (2000) 331.
5 E. Kymakis, I. Alexandou and G. A. J. Amaratunga, Synth. Met., 127 (2002) 59.
6 N. Grossiord, J. Loos, O. Regev and C. E. Koning, Chem. Mater., 18 (2006) 1089.
7 T. W. Ebbesen and P. M. Ajayan, Nature, 358 (1992) 220.
8 A. Thess, R. Lee, P. Nikolaev, H. Dai, P. Petit, J. Robert, C. Xu, Y. H. Lee, S. G. Kim, A. G. Rinzler, D. T. Colbert, G. E. Scuseria, D. Tomanek, J. E. Fisher and R. E. Smalley, Science, 273 (1996) 483.
9 V. Ivanov, J. B. Nagy, P. Lambin, A. Lucas, X. B. Zhang, X. F. Zhang, D. Bernaerts, G. Van Tendeloo, S. Amelinckx and J. Van Landuyt, Chem. Phys. Lett., 223 (1994) 329.
10 C. Journet, W. K. Maser, P. Bernier, A. Loiseau, M. Lamy de la Chapelle, S. Lefrant, P. Deniard, R. Lee and J. E. Fischer, Nature, 388 (1997) 756.
11 M. E. Itkis, D. E. Perea, R. Jung, S. Niyogi and R. C. Haddon, J. Am. Chem. Soc., 127 (2005) 3439.
12 M. E. Itkis, D. E. Perea, S. Niyogi, J. Love, J. Tang, A. Yu, C. Kang, R. Jung and R. C. Haddon, J. Phys. Chem. B, 108 (2004) 12770.
13 J. Gavillet, A. Loiseau, F. Ducastelle, S. Thair, P. Bernier, O. Stéphan, J. Thibault and J.-C. Charlier, Carbon, 40 (2002) 1649.
14 M. T. Martinez, M. A. Callejas, A. M. Benito, M. Cochet, T. Seeger, A. Anson, J. Schreiber, C. Gordon, C. Marhic, O. Chauvet, J. L. G. Fierro and W. K. Maser, Carbon, 41 (2003) 2247.
15 N. Grossiord, O. Regev, J. Loos, J. Meuldijk and C. E. Koning, Anal. Chem., 77 (2005) 5135.
16 B. K. Pradhan, A. R. Harutyunyan, D. Stojkovic, J. C. Grossman, P. Zhang, M. W. Cole, V. Crespi, H. Goto, J. Fujiwara and P. C. Eklund, J. Mater. Res., 17 (2002) 2209.
17 C. A. Furtado, U. J. Kim, H. R. Gutierrez, L. Pang, E. C. Dickey and P. C. Eklund, J. Am. Chem. Soc., 126 (2004) 6095.

18 U. J. Kim, C. A. Furtado, X. Liu, G. Chen and P. C. Eklund, J. Am. Chem. Soc., 127 (2005) 15437.
19 A. C. G. Dillon, T. K. M. Jones, J. L. Alleman, P. A. Parilla and M. J. Heben, Adv. Mater., 11 (1999) 1354.
20 D. Bom, R. Andrews, D. Jacques, J. Anthony, B. Chen, M. S. Meier and J. P. Selegue, Nano Letters, 2 (2002) 615.
21 H. Hu, B. Zhao, M. E. Itkis and R. C. Haddon, J. Phys. Chem. B, 107 (2003) 13838.
22 H. Kajiura, S. Tsutsui, H. Huang and Y. Murakami, Chem. Phys. Lett., 364 (2002) 586.
23 S. Arepalli, P. Nikolaev, O. Gorelik, V. G. Hadjiev, W. Holmes, B. Files and L. Yowell, Carbon, 42 (2004) 1783.
24 S. Scaccia, M. Carewska, and P. P. Prosini, Thermochim. Acta, 435 (2005) 209.
25 X. L. Xie, K. Aloys, X. P. Zhou and F. D. Zeng, J. Therm. Anal. Cal., 74 (2003) 317.
26 H. Yu, C. Lu, T. Xi, L. Luo, J. Ning and C. Xiang, J. Therm. Anal. Cal., 82 (2005) 97.
27 Z. Konya, T. Kanyo, A. Hancz and I. Kiricsi, J. Therm. Anal. Cal., 79 (2005) 567.
28 P. S. Gill, S. R. Sauerbrunn and B. S. Crowe, J. Thermal Anal., 38 (1992) 255.
29 Y. Xi, W. Martens, H. He and R. L. Frost, J. Therm. Anal. Cal., 81 (2005) 91.
30 C.-H. Kiang, W. A. Goddard III, R. Beyers and D. S. Bethune, in Carbon nanotubes, Ed. by M. Endo, S. Iijima and M. S. Dresselhaus, Pergamon, Oxford 1996, pp. 47–58.
31 V. Ivanov, A. Fonseca, J. B. Nagy, A. Lucas, P. Lambin, D. Bernaerts and X. B. Zhang, in Carbon nanotubes, Ed. by M. Endo, S. Iijima and M. S. Dresselhaus, Pergamon, Oxford 1996, pp. 15–26.
32 J.-O. Muller, D. S. Su, R. E. Jentoft, J. Kohnert, F. C. Jentoft and R. Schlogl, Catalysis Today, 102–103 (2005) 259.
33 L. S. K. Pang, J. D. Saxby and S. P. Chatfield, J. Phys. Chem., 97 (1993) 6941.
34 M. R. Smith Jr., S. W. Hedges, R. LaCount, D. Kern, N. Shah, G. P. Huffman and B. Bockrath, Carbon, 41 (2003) 1221.
35 I. W. Chiang, B. E. Brinson, R. E. Smalley, J. L. Margrave and R. H. Hauge, J. Phys. Chem. B, 105 (2001) 1157.

Received: March 2, 2006
Accepted: June 20, 2006
OnlineFirst: February 13, 2007

DOI: 10.1007/s10973-006-7563-9